

Study on the Mechanism of the Formation of Polyhedral Oligomeric Silsesquioxanes by the 2D Correlation Infrared Spectral

Yanbin Qu, Guangsu Huang, Xiaoran Wang, Jiali Li

College of Polymer Science and Engineering, State Key Laboratory of Polymer Materials Engineering, Sichuan University, Chengdu 610065, China

Received 7 July 2011; accepted 14 November 2011

DOI 10.1002/app.36489

Published online in Wiley Online Library (wileyonlinelibrary.com).

ABSTRACT: Synthesis of polyhedral oligomeric silsesquioxanes (POSS) by the hydrolytic condensation reaction of trifunctional organosilanes [e.g., RSiCl_3 or RSi(OR)_3] may have achieved success. However, the exact formation mechanism of POSS, especially, an evolution process in the reaction still remains unclear. In this work, a real-time FTIR was carried out to trace the synthesis process of POSS. It was found that linear siloxanes, cyclic siloxanes, and cage-like polysiloxanes were formed during the reaction. With the help of generalized two-dimensional (2D) correlation analysis, we obtained exact sequential change among the three siloxanes, with the linear siloxanes formed initially. Following this was the emergence of cyclic silox-

anes, and finally the cage-like polysiloxanes. Consequently, we not only proved the existence of the linear and cyclic siloxanes but also accurately detected the sequential change of the siloxanes in the process, which exhibited an intact and visual evolution process of POSS formation. Based on this, the reaction mechanism is presented. Finally, the chemical structure of cage-like products was further characterized by $^{29}\text{Si-NMR}$ and GPC measurements. © 2012 Wiley Periodicals, Inc. *J Appl Polym Sci* 000: 000–000, 2012

Key words: POSS formation; mechanism; FTIR spectroscopy; two-dimensional correlation analysis

INTRODUCTION

Polyhedral oligomeric silsesquioxanes (POSS) and some related compounds have attracted considerable interests for many years because of their variety of practical uses in biomaterials,¹ atomic oxygen-resistant coatings,^{2,3} additives in high temperature-resistant composites,⁴ and photoluminescence materials. The incorporation of nanosize POSS cores into a polymer matrix can result in significant improvements in a variety of physical and electrical properties. For example, Xiao et al.⁵ first introduced silsesquioxane materials to organic light emitting diodes (OLEDs) in 2003. They covalently anchored POSS at the chain-terminal of poly (phenylene vinylene) to obtain the higher brightness and external quantum efficiency OLEDs materials. In addition, POSS can also be used to improve the dielectric property of polymer materials. S. Devaraju⁶ prepared polyhedral oligomeric silsesquioxane (POSS)-polyimide (PI) hybrid nanocomposites from ether linked cyclohexyl

diamine(ELCD)-modified polyamic acid (PAA) with POSS derivative of octaaminophenylsilsesquioxane (OAPS). From the dielectric studies, it was found that compared with those of neat PI, the increasing percentage concentration of OAPS into the PI network exhibited a striking decreasing trend in the values of dielectric constant.

At present, many methods of preparing POSS have been proposed, which can be roughly classified into two types: one is making POSS species by the controlled hydrolysis and condensation of organotrichlorosilanes and the other is chemically modifying the functional groups of an already existing POSS core to obtain a new POSS derivative. In the study, we adopt the first method which has been widely used to prepare POSS. However, the mechanism of POSS formation, especially, an evolution process in the reaction still remains unclear since the reaction is rather complicated. An intensive understanding and mastery of the synthesis mechanism of POSS is necessary for us to create new species of POSS and control the intermediate process and structure for achieving ideal yield. Accordingly, some researchers have attempted to solve the problem. Takako Kudo^{7–9} once employed an *ab initio* molecular orbital for studying the synthesis mechanism of POSS. They found that the energy barrier in the hydrolysis and initial condensation processes can be overcome through hydrogen bonding with water to

Correspondence to: G. Huang (guangsu-huang@hotmail.com).

Contract grant sponsor: National Science of Foundation of China (NSFC); contract grant number: 51073097.

stabilize the transition state in terms of second-order perturbation theory (MP2)³ and the coupled cluster method. This depiction might be reasonable. However, it was completely based on theoretical calculation and lacked experimental support. Latter, X-ray measurement ascertained the structure of POSS, from which the mechanism^{10–12} of POSS formation was deduced inversely. Unfortunately, the formation mechanism is still deduced by theory because the process could not be real-time detected by valid experiment.

Fourier Transform infrared spectroscopy (FTIR) as a technique for analyzing the molecular structures, especially crosslinking structures, has been proved to be a powerful tool to follow the reaction mechanism. However, some of the peaks in FTIR spectra are difficult to clearly assign due to the overlapped peaks resulting from simultaneous occurrence of a variety of fundamental transitions in the hydrolytic condensation reaction. Therefore, the development of powerful techniques for unraveling the complicated spectra has long been attempted.

Recently, generalized two-dimensional (2D) correlation analysis^{13,14} which was first introduced by Noda in 1993¹⁵ can handle spectral fluctuations as an arbitrary function of time or any other physical variable. Based on time-resolved FTIR signals, it has been applied to analyze the inter- and intramolecular interaction. 2D correlation spectroscopy is powerful in distinguishing vague band assignments which enhances apparent spectral resolution efficiently. Specially, it can provide more information about the variation orders of the spectral intensity from different functional groups by analyzing the synchronous and asynchronous corresponding spectra. For instance, Liang Li¹⁶ monitored the isothermal curing process of diglycidyl ether of bisphenol A (DGEBA) cured with 4, 4'-diaminodiphenylmethane (DDM) *in situ* by mid-infrared and near-infrared spectroscopy and obtained the curing mechanism by generalized 2D correlation analysis. Xiaoyun Liu et al.¹⁷ investigated the curing reaction of the blends of bisphenol A dicyanate ester (BADCy) and 4, 4'-bismaleimidodiphenylmethane (BMI) by using generalized 2D correlation analysis. Above results showed whether adding the catalysis or not could lead apparently to different curing mechanisms. Examples above demonstrate that 2D correlation analysis is especially effective for analyzing cross-linking reaction mechanism which could not be achieved by employing other analysis methods.

As far as we are aware, 2D heterospectral correlation has not been employed in the hydrolytic condensation process of trifunctional organosilanes to prepare POSS. In this article, a real-time FTIR tracing to the hydrolytic condensation process for preparing POSS is carried out, and the detailed process is

described based on 2D correlation analysis. From the experimental results, we first present the reaction mechanism of POSS formation from valid experiment analysis.

EXPERIMENTAL

Materials

Phenyltrimethoxysilane (>98%) was purchased from Liyang Tomorrow Chemical and used without further purification. Sodium hydroxide (AR) was used as received. 2-propyl alcohol (AR) was purified by 4A molecular sieve before being used.

Fourier transform infrared spectroscopy measurements

The hydrolytic condensation reaction was performed in a sample cell, which was constructed for kinetic measurements. Totally, 0.1 g of a mixture of phenyltrimethoxysilane (24 g, 0.12 mol), sodium hydroxide (3.2 g, 0.08 mol), water (2.5 g, 0.14 mol), and 2-propyl alcohol (100 mL) were sandwiched between two CaF₂ windows which sealed with dried nitrogen, and the thickness of it was 27 μm. The windows were located in Heated cell (HT-32), which was attached to a Raman spectrometer (Nicolet IS 10). The estimated spectral resolution was 4 cm⁻¹ and the number of scans was 32. The investigated bands scope between 1500 cm⁻¹ and 1000 cm⁻¹ correspond to Si—OCH₃ and Si—O—Si stretching vibration.

The hydrolysis was started in the sample cell by heating to 90°C. During the reaction, Raman spectra with an acquisition time of 0.5 min were recorded.

Characterization

²⁹Si-NMR analysis was measured on a Bruker AV 11-400 spectrometer. The sample was dissolved in heavy chloroform (CDCl₃) and the solution was measured with tetramethylsilane (TMS 0 ppm) as an internal standard substance; Gel permeation chromatography (GPC) was performed on a HLC-8320GPC system, using an EcoSEC RI detector and EcoSEC Styragel columns [Super HM-H*2(6.0 mm × 15 cm)]. The system was calibrated using polystyrene standards. Tetrahydrofuran (THF) was used as the eluent, at a flow rate of 0.6 mL/min.

Two-dimensional infrared correlation analysis

Sixteen spectra at equal time intervals in a certain wavenumber range were drawn for application of 2D correlation analysis by using 2D Shige software. Time-averaged one-dimensional (1D) reference spectrum is provided at the top of the 2D maps. In the 2D correlation maps, unshaded regions indicate positive cross peaks, while shaded regions indicate negative cross peaks.

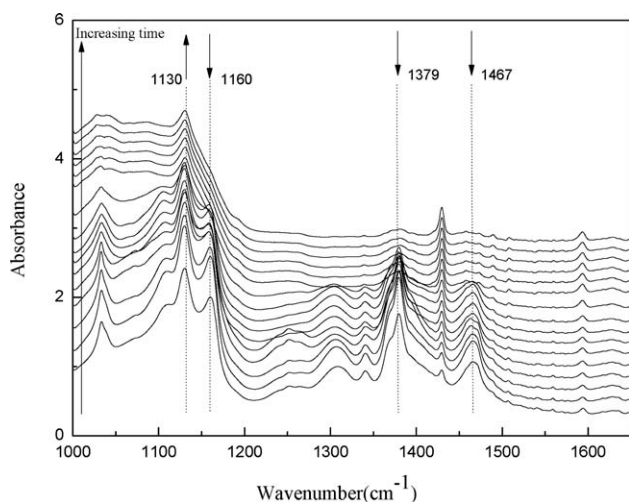


Figure 1 FTIR spectra of the hydrolytic condensation of trifunctional organosilanes. The arrows presented in the figure indicate the increase or decrease of the intensities of bands during the hydrolysis.

RESULTS AND DISCUSSION

Figure 1 shows the typical real-time FTIR spectra tracing to the hydrolytic condensation of trifunctional organosilanes. In the FTIR spectra, peaks at 1379, 1467, 2971, and 2935 cm^{-1} can be assigned to the C—H

TABLE I
Tentative Assignments of Spectral Bands

Position cm^{-1}	Assignments (tentative)
1080	Si—O—Si cyclic polysiloxanes asym. Str.
1594	Si—Ph Si—C bending
1125	Si—Ph Si—C Str.
1429	Ph C=C Str.
2935, 1379, 1467, 2971	Si—O—CH ₃ C—H Str.
1100	Si—O—Si (linear siloxanes) asym. Str.
1130	Si—O—Si (cage siloxanes) asym. Str.

Str, stretch; sym, symmetric; asym, asymmetric.

stretching vibrations of Si—OCH₃ groups. The overlapped peaks from 1080 to 1130 cm^{-1} are attributed to the Si—O—Si superposition of cyclic siloxanes, linear siloxanes, and cage-like polysiloxanes.

More detailed band assignments are listed in Table I. To perform further analysis, the results shown in Figure 2 were calculated by the integral of four typical bands, centered at 1467, 1100, 1080, and 1130 cm^{-1} in the FTIR region, which were used to analyze the hydrolytic condensation process of trifunctional organosilanes to forming cage-like POSS.

The hydrolytic condensation reaction can be separated into four steps according to reaction time.

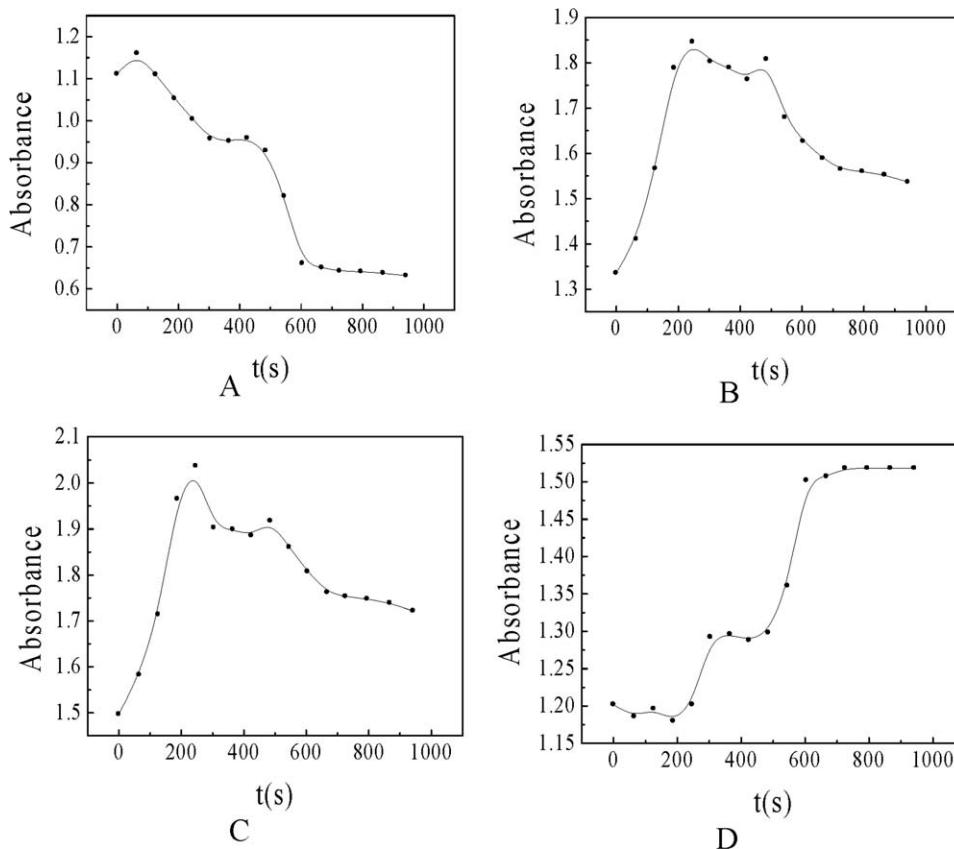


Figure 2 Absorbance of typical bands during the reaction. A: The band centered at 1467 cm^{-1} ; B: The band centered at 1100 cm^{-1} ; C: The band (cyclic siloxanes) centered at 1080 cm^{-1} ; D: The band centered at 1130 cm^{-1} (cage-like polysiloxanes).

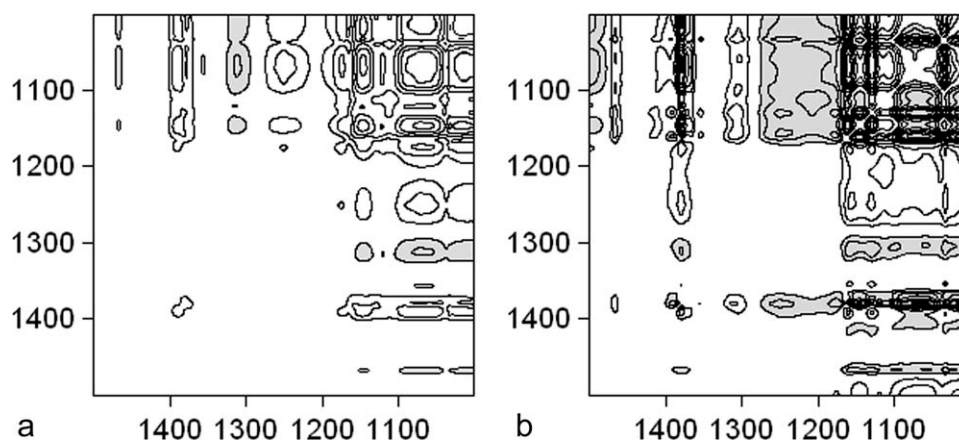


Figure 3 2D correlation spectra derived from the FTIR spectra of the reaction before 245 s. A: Synchronous spectrum; B: Asynchronous spectrum; Negative peaks are marked by shading.

Before 188 s, it can be found that the absorbance of the band at 1467 cm^{-1} decreases rapidly upon the hydrolytic process and the bands at 1080 and 1100 cm^{-1} increase during the condensation process, which reveals the high consumption rate of methoxy groups in the initial stage of hydrolytic process. In addition, condensation reaction occurs almost simultaneously with the hydrolysis reaction, during which the linear siloxanes and cyclic siloxanes form immediately and both amounts increase rapidly, but the reaction rate of condensation is slightly faster than that of hydrolysis.

The time between 188 and 304 s is a hydrolysis constant rate period. The rate of condensation decreases, when the rate of hydrolysis remains nearly unchanged. At the same time, the bands at 1100 and 1080 cm^{-1} go down rapidly in intensity, which shows that the quantities of linear and cyclic siloxanes reduce. Furthermore, the bimodal peaks of phenyltrimethoxysilane at 1129 and 1160 cm^{-1} begin to transform to the unimodal peak at 1130 cm^{-1} whose intensity increases rapidly suggesting that cage-like polysiloxanes are formed.

An equilibrium period appears between the time of 304 and 485 s when the rate of hydrolysis and condensation become slower and the amounts of the products remain unchanged. This is attributed to the fact that the decline of hydrolysis rate might be caused by a shortage of water which would lead to a lack of hydroxyl groups and therefore inhibit hydrolysis from further happening.

After 485 s, the increased rate of hydrolysis subsequently would be explained by the starting condensation which liberates new water molecules, accordingly, the condensation rate of cage-like polysiloxanes increases rapidly. In the meantime, the bands at 1467, 1100, and 1080 cm^{-1} in intensity decrease while the band at 1130 cm^{-1} in intensity increases more rapidly.

From the results of FTIR, we can find the appearance and disappearance of methoxy groups, linear siloxanes, cyclic siloxanes, and cage-like polysiloxanes during the reaction. However, we still could not distinguish the variation sequence among the four groups, so it is difficult to find a relationship between them. To further resolve the problems, we used 2D correlation spectra as the analytical method to study the orders of the band changes at 1467, 1100, 1080, and 1130 cm^{-1} , which represent the absorbance band of Si—OCH₃ groups, the Si—O—Si of linear siloxanes, cyclic siloxanes and cage-like polysiloxanes, respectively, during the reaction.

Generalized 2D correlation spectra on the evolution of FTIR spectra of the POSS formation are presented in Figures 3 and 4. According to the publications of Noda,¹⁵ the synchronous 2D correlation represents the simultaneous or coincidental changes of spectral intensities of cross peaks [$\psi(v_1, v_2)$]. The sign of cross peaks becomes positive (unshaded area) if the spectral intensities at corresponding wavenumbers are either increasing or decreasing together as functions of the external variable during the observation interval. On the contrary, the negative sign (shaded area) of cross peaks indicates that one of the spectral intensities is increasing while the other is decreasing. In the asynchronous spectrum, the dynamic spectral intensity variations represent sequential, or unsynchronized, changes of spectral intensities measured at band v_1 and band v_2 . Namely, the intensity of the asynchronous cross peak $\psi(v_1, v_2)$ is able to give information about the sequential order of intensity changes between band v_1 and band v_2 . The sign of an asynchronous cross peak [$\psi(v_1, v_2)$] is positive if the band v_1 varies prior to band v_2 . On the contrary, if band v_1 varies after band v_2 , the cross peak [$\psi(v_1, v_2)$] is negative. The above rule, however, is reversed if the sign of a

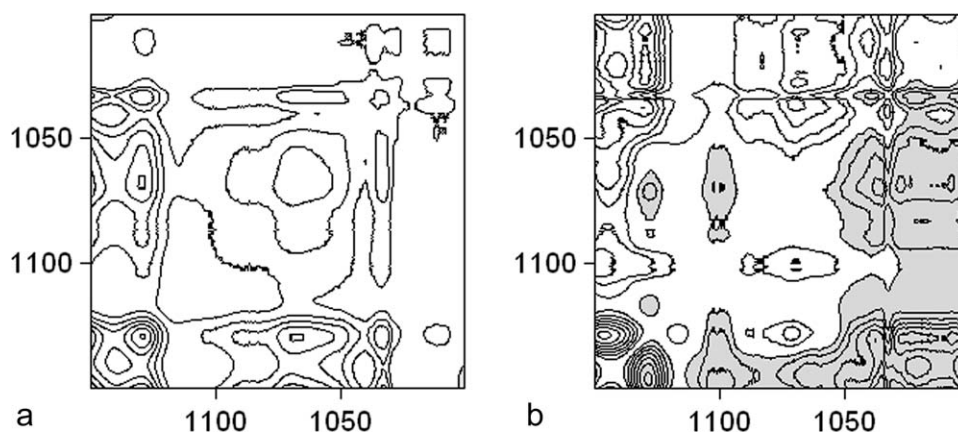


Figure 4 2D correlation spectra derived from the FTIR spectra of the reaction between 245 and 604 s. A: Synchronous spectrum; B: Asynchronous spectrum; Negative peaks are marked by shading.

synchronous peak at the same coordinate [$\psi(v_1, v_2)$] is negative.

Figure 3 shows synchronous and asynchronous correlation spectra of the system in the region of 1000–1500 cm^{-1} during the reaction before 245 s. In the synchronous 2D spectrum [Fig. 3(A)], three autopeaks at 1467, 1100, and 1080 cm^{-1} can be found, which indicates the significant changes of Si—OCH₃ bands, Si—O—Si bands (linear siloxanes) and Si—O—Si bands (cyclic siloxanes). Also, another two distinct cross peaks observed on the upper left side of the correlation spectrum are $\psi(1467, 1100 \text{ cm}^{-1})$ and $\psi(1467, 1080 \text{ cm}^{-1})$, respectively, which are all negative. These peaks, combined with Figure 2(A–C), demonstrate that the bands at 1100 and 1080 cm^{-1} respecting the Si—O—Si overtones of linear siloxanes and cyclic siloxanes increase, while the bands at 1467 cm^{-1} representing OCH₃ group decrease during the reaction.

In the corresponding asynchronous 2D spectrum [Fig. 3(B)], two positive cross peaks, $\psi(1467, 1100 \text{ cm}^{-1})$ and $\psi(1100, 1080 \text{ cm}^{-1})$ can be identified, which can be attributed to vibrations of Si—OCH₃ and Si—O—Si bands in both of linear and cyclic siloxanes respectively. On the basis of Noda's rule, the order of the band intensity changes accords with the following sequence: 1467 > 1100 > 1080 (" $>$ " means "prior to"), which means that Si—OCH₃ hydrolyzes firstly and is followed by linear siloxanes, finally cyclic siloxanes are generated.

Figure 4 shows synchronous and asynchronous correlation spectra of the system in the region of 1000–1150 cm^{-1} during the reaction between 245 and 604 s. In the synchronous 2D spectrum [Fig. 4(A)], three autopeaks appear at 1100, 1080, and 1130 cm^{-1} and two positive cross peaks, $\psi(1130, 1100 \text{ cm}^{-1})$ and $\psi(1130, 1080 \text{ cm}^{-1})$ as well as their change rules are found, which demonstrate that the peaks at 1130, 1100, and 1080 cm^{-1} vary with the same tendency, whereas an complete opposite result

is obtained from Figure 2(B–D). This phenomenon can be well explained by the fact that the bands around 1100 and 1080 cm^{-1} are totally overlapped by the band around 1130 cm^{-1} , thus the decreases of Si—O—Si band intensity of linear and cyclic siloxanes are nearly covered by the increase of intensity of cage-like polysiloxanes, which also leads to the occurrence of two positive cross peaks in the synchronous 2D spectrum.

In the corresponding asynchronous 2D spectrum [Fig. 4(B)], two negative cross peaks, $\psi(1130, 1080 \text{ cm}^{-1})$ and $\psi(1100, 1130 \text{ cm}^{-1})$ can be found. On the basis of Noda's rule, the changes of band intensity follow the sequence: 1080 > 1130, 1130 > 1100 (" $>$ " means "prior to"). It means that the change of cyclic siloxanes is prior to that of cage-like polysiloxanes, while the change of cage-like polysiloxanes is prior to that of linear siloxanes. These results, combined with Figure 2(B–D) and synchronous 2D spectrum, indicate that great quantities of cage-like polysiloxanes are formed at the expense of the cyclic siloxanes. Besides, only small quantities of cage-like polysiloxanes are split by NaOH, which results in the formation of a few linear siloxanes.

From the results of the 2D correlation analysis, we can present the POSS synthesis mechanism as depicted in Figure 5.

In the first step, an alkaline intermediate A is generated from hydrolysis of phenyltrimethoxysilane under H₂O and NaOH. At this moment, there is equilibrium between A and B. Second, alkaline intermediate A and B as template center can cause siloxanes rearrangement resulting in the formation of cyclic siloxanes D.¹⁸ Reasonably, during the rearrangement and oligocyclization process, the linear siloxanes intermediate C is formed inevitably. At last, the cage-like polysiloxanes E can form based on two stereoregular cyclic siloxanes D. The structures and yields of these cage-like polysiloxanes¹⁹ certainly depend upon the nature of the alkaline metal,

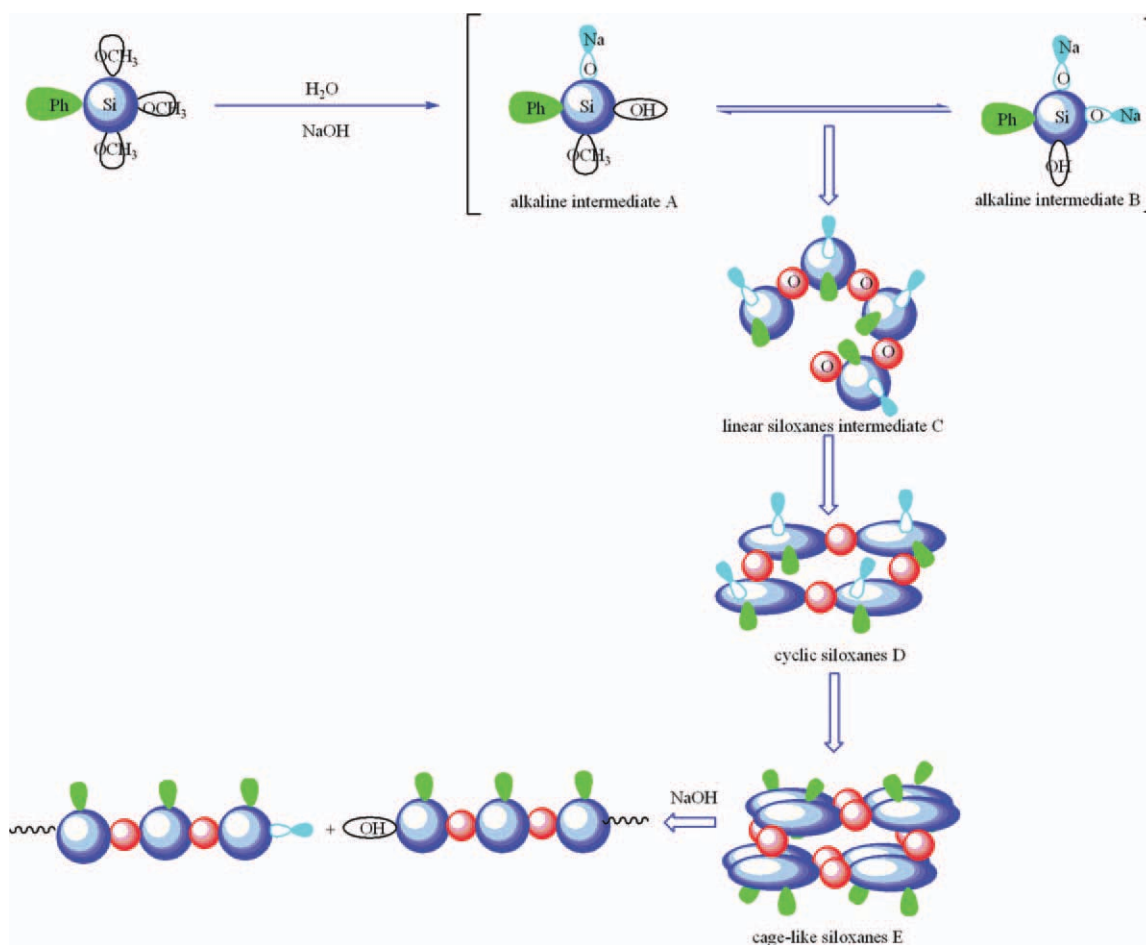


Figure 5 Plausible forming mechanism of POSS from hydrolysis and condensation reaction.

the reactivity of alkoxy groups, the amount of water and the nature of the solvent. By controlling reaction conditions, the products can be synthesized selectively. During the reaction, the rearrangement and oligocyclization programs, proposed by J. F. Hyde, etc.¹⁸ in 1953, are key and quite complex. As for the rearrangement process, many related researches^{20–23} also indicated that the numbers of siloxane rings selectively depended on different conditions. Although

above researches mentioned the oligocyclization, the cyclic siloxanes are all imaginary by theory speculation and never be detected in the practical process because of the rapid hydrolysis reaction.

In fact, no one has ever found the medial process when POSS is formed. In this study, we monitor the groups change process by real-time FTIR spectroscopy and accurately detect the sequential order of the group intensity changes by 2D correlation

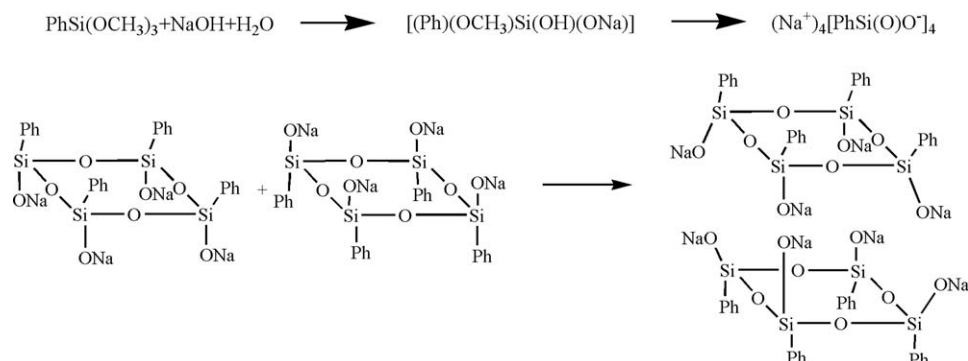


Figure 6 The reaction equation of POSS formation.



Figure 7 Splitting reaction of POSS by NaOH.

analysis, which exhibits an intact and visual evolution process of POSS formation. Our work also proves that oligocyclization process is inevitable when producing cage-like polysiloxanes and offers valid experimental proof for the oligocyclization assumption.

An idiographic reaction equation is shown below in the text. Reasonably, alkaline can not only catalyze the formation of cage-like polysiloxanes but also split the siloxane bonds of the polysiloxanes in an alcohol media. It is believed that the reaction takes place by virtue of an initial cleavage of the siloxane bond by NaOH to form a sodium silanolate group and a silanol group. The reaction scheme is shown below in Figure 7.

To further confirm the structure of above cage-like polysiloxanes, GPC and ^{29}Si NMR analyses are carried out (Figs. 8 and 9). For the sake of avoiding the intermediate product with active sodium atom changing during the characterization, we hydrolyzed the above intermediate product to obtain the product represented in Figure 9. Accordingly, by the characterization of the product represented in Figure 9, we judged that the product before hydrolysis has a structure represented in Figure 6.

From Figure 8, it can be seen that the product exhibits predominantly one peak and has a weight average molecular weight (M_w) of 1008 and a number average molecular weight (M_n) of 980, which shows a very fine monodispersibility.

In the ^{29}Si NMR chart (Fig. 9), three peaks of one peak originating in a Si—OH group in -63 ppm and two peaks originating in a T structure having a phenyl group in -77.8 and -78.4 ppm in a ratio of 2 : 1.

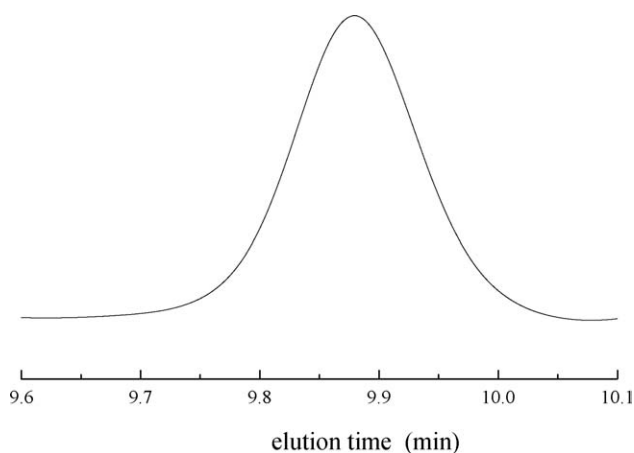


Figure 8 GPC of the products of the model reaction.

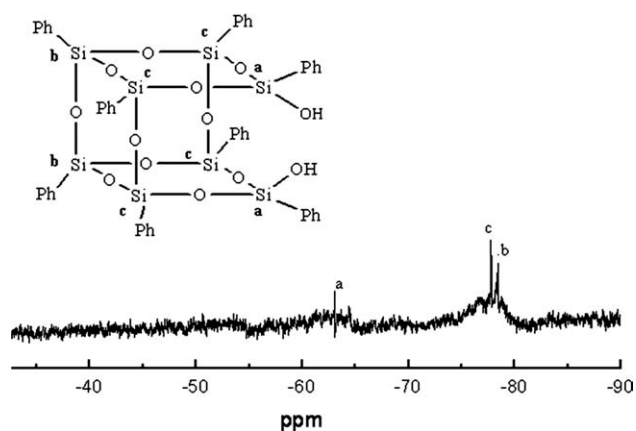


Figure 9 ^{29}Si NMR of the products of the model reaction.

The T structure is a structure in which Si is bonded to three Os. The result, combined with GPC, shows that the matter described above has a structure represented by Figure 9 in this experimental conditions.

CONCLUSION

Real-time tracing of FTIR and 2D hetero-spectral correlation are very powerful analytical methods to obtain and distinguish superposed distributing bands, which provide exact information about the specific order of the absorbing band changes. In the article, 2D hetero-spectral correlation analysis is applied to study the mechanism of POSS formation successfully. According to the results, we propose the mechanism that during the sodium hydroxide catalyzing the hydrolytic condensation of trifunctional organosilanes, sodium silanolate intermediates are formed first, then it undergoes oligocyclization resulting in the formation of cyclic siloxanes, and finally a great number of cage-like polysiloxanes are formed. It furthermore indicates that the generations of cage-like polysiloxanes derive from cyclic siloxanes directly. Meanwhile, sodium hydroxide can also split the siloxanes' bonds of the polysiloxanes resulting in the formation of a few linear siloxanes. ^{29}Si NMR and GPC analyses further confirm the structure of the polysiloxanes.

References

1. Lligadas, G.; Ronda, J. C.; Galià, M.; Cádiz, V. *Biomacromolecules* 2006, 7, 3521.
2. Hoflund, G. B.; Gonzalez, R. I.; Phillips, S. H. *J Adhes Sci Technol* 2001, 15, 1199.
3. Gonzales, R. I.; Phillips, S. H.; Hoflund, G. B. *J Spacecr Rockets* 2000, 37, 463.
4. Feher, F. J.; Newman, D. A. *J Am Chem Soc* 1990, 112, 1931.
5. Xiao, S.; Nguyen, M.; Gong, X.; Cao, Y.; Wu, H. B.; Moses, D.; Heeger, A. *Adv Funct Mater* 2003, 13, 25.
6. Devaraju, S.; Vengatesan, M. R.; Alagar, M. *High Performance Polym* 2011, 23, 99.

7. Kudo, T.; Gordon, M. S. *J Phys Chem A* 2000, 104, 4058.
8. Kudo, T.; Machida, K. *J Phys Chem A* 2005, 109, 5424.
9. Kudo, T.; Gordon, M. S. *J Phys Chem A* 2002, 106, 11347.
10. Olga, I. S.; Pozdnyakova, Y. A.; Yulia, A. M.; Korin, S. D.; Bukalov, S. S.; Leites, L. A.; Lyssenko, K. A.; Peregudov, A. S.; Auner, N.; Katsoulis, D. E. *Inorg Chem* 2002, 41, 6892.
11. Shchegolikhina, O.; Ozdniakova, Y.; Antipin, M. *Organometallics* 2000, 19, 1077.
12. Molodtsova, Y. A.; Pozdnyakova, Y. A.; Lyssenko, K. A.; Blagodatskikh, I. V.; Katsoulis, D. E.; Shchegolikhina, O. I. *J Organomet Chem* 1998, 571, 31.
13. Noda, I. *Vib Spectrosc* 2004, 36, 143.
14. Noda, I. *J Mol Struct* 2006, 799, 2.
15. Noda, I. *Appl Spectrosc* 1993, 47, 1329.
16. Li, L.; Wu, Q.; Li, S.; Wu, P. *Appl Spectrosc* 2008, 62, 1129.
17. Liu, X.; Yu, Y.; Li, S. *Polymer* 2006, 47, 3767.
18. Hyde, J. F. U.S. Pat. 2,634, 284, 1953.
19. Igonin, V. A.; Shchegolikhina, O. I.; Lindeman, S. V.; Levitsky, M. M.; Srtuchkov, Y. T.; Zhdanov, A. A. *J Organomet Chem* 1992, 423, 351.
20. Shchegolikhina, O. I.; Zhdanov, A. A.; Igonin, V. A.; Ovchinnikov, Yu. E.; Shklover, V. E.; Struchkov, Y. T. *Organomet Chem USSR* 1991, 4, 39.
21. Igonin, V. A.; Lindeman, S. V.; Potekhin, K. A.; Shklover, V. E.; Struchkov, Y. T.; Shchegolikhina, O. I.; Zhdanov, A. A.; Razumovskaya, I. V. *Organomet Chem* 1991, 4, 383.
22. Igonin, V. A.; Lindeman, S. V.; Struchkov, Y. T.; Shchegolikhina, O. I.; Zhdanov, A. A.; Molodtsova, Y. A.; Razumovskaya, I. V. *Organomet Chem* 1991, 4, 672.
23. Igonin, V. A.; Shchegolikhina, O. I.; Lindeman, S. V.; Levitsky, M. M.; Srtuchkov, Y. T.; Zhdanov, A. A. *J Organomet Chem* 1992, 423, 351.